Article

A Novel Data Acquisition System for Obtaining Thermal Parameters of Building Envelopes

Behnam Mobaraki [1],*, Seyedmilad Komarizadehasl [2], Francisco Javier Castilla Pascual [3],
José Antonio Lozano-Galant [1] and Rocio Porras Soriano [4]

1 Department of Civil and Building Engineering, Universidad de Castilla-La Mancha (UCLM),
Av. Camilo Jose Cela s/n, 13071 Ciudad Real, Spain; joseantonio.lozano@uclm.es
2 Department of Civil Engineering and Environmental Engineering, Universitat Politècnica de Catalunya
BarcelonaTech (UPC), C/Jordi Girona 1-3, 08034 Barcelona, Spain; milad.komary@upc.edu
3 Department of Civil and Building Engineering, Universidad de Castilla La Mancha (UCLM),
MAEE-UCLM Research Group, Escuela Politécnica de Cuenca, Campus Universitario,
16071 Cuenca, Spain; fcojavier.castilla@uclm.es
4 Department of Applied Mechanics and Projects Engineering, Universidad de Castilla-La Mancha (UCLM),
Av. Camilo Jose Cela s/n, 13071 Ciudad Real, Spain; rocio.porras@uclm.es
* Correspondence: behnam.mobaraki@uclm.es

Abstract: Owing to the high energy consumption in the building sector, appraising the thermal performance of building envelopes is an increasing concern. Recently, a few in situ methodologies to diagnose the thermal parameters of buildings have been considered. However, because of their limitations such as low accuracy, limited number of measurements, and the high cost of monitoring devices, researchers are seeking a new alternative. In this study, a novel hyper-efficient Arduino transmittance-meter was introduced to overcome these limitations and determine the thermal parameters of building envelopes. Unlike conventional methodologies, the proposed transmittance-meter is based on synchronized measurements of different parameters necessary to estimate the transmittance parameter. To verify the applicability of the transmittance-meter, an experimental study was conducted wherein a temperature-controlled box model was thermally monitored, and the outputs of the transmittance-meter employed were compared with those captured by a commercial device. The results revealed a high level of reduction in cost and a low range of difference compared with the latter, thereby validating the applicability of the proposed thermal monitoring system.

Keywords: HEAT; building thermal monitoring; temperature-based method; energy efficiency; transmittance parameter; low-cost sensors

1. Introduction

Buildings waste high amounts of energy mainly because of their age and poor insulation. Currently, energy consumption by buildings contributes up to 31% of the total energy demand worldwide [1]. Since 1990, energy consumption in the building sector in Europe has tended to increase by an average of 1% annually. This rate of consumption varies based on age and geographical location. For instance, in Spain, the Andalusian Energy Agency announced a 4.1% increase in energy in residential buildings from 2014 to 2016 [2], while the energy consultancy of Barcelona declared a 15% energy savings rate from 2000 to 2010 [3]. The primary use of energy in buildings goes toward heating, cooling, cooking, and appliances. Since 2011, approximately 81% of the energy generated for these needs has been obtained from fossil fuels [4]. The energy scape in buildings mostly depends on the following factors: (1) building envelopes (including roofs, sub-floors, doors, windows, and walls); according to the United States Energy Information Administration, 25% of heat loss comes from attics, 15% from basements/floors, 35% from walls, and 25% from windows/doors [5], and (2) thermal bridges (including wall to wall, wall to door, wall to

window, and wall to floor junctions) [6]. It has been stated that thermal bridges in regular buildings attenuate the effectiveness of insulation by 40% [7]. Therefore, characterizing the actual thermal parameters of building envelopes has become a main concern for building engineers [8]. Examples of thermal monitoring of different elements of a building (including walls, floors, ceilings, and window glass) are provided in [9]. As windows are a main contributor to the energy scape in the building sector, diagnosing the thermal parameters of them has become a key research subject [10]. Table 1 lists previous studies that have been conducted to derive the transmittance parameter (U-value) of different types of windows (connected with diverse frames) using numerical and experimental techniques.

Table 1. Previous studies for deriving the U-value of different types of windows using different techniques.

Application	Method/Sensor	Number of Sensors	Reference
Windows and built- up panels	GHB [1]	2	[11]
Window	GHB and FEM [2]	16	[12]
Wooden windows	ANN [3]	-	[13]
Single window glazing	GHB	5	[14]
Window (steel frame)	CHB [4]	3	[15]
Window frames	ANSYS CFD/GAMBIT	-	[16]

[1] GHB: Guarded hot box. [2] FEM: Finite element method. [3] ANN: Artificial neural network. [4] CHB: Calorimetric hot box.

An accurate evaluation of building thermal performance is achieved by calculating the U-value. A low U-value represents a better insulated structure. This parameter is used to appraise annual energy loss in the building sector. The U-value of multilayered building walls was traditionally determined using a destructive method of measuring the thickness of each layer and then assigning conductivity values to each layer. To accomplish this, it was necessary to core the wall and add the resistance values (R-value) of the individual layers. However, inferring the thermal parameters of a structure using this method results in uncertainties regarding measurements of thickness, and the identification of material properties that might not be accurately connected to the actual performance of the building elements. Nevertheless, this approach was widely implemented in accordance with ISO 6946 guidelines. However, recent research has standardized U-value estimation by presenting various techniques such as heat flux meter (HFM) method [17], temperature control box heat flux meter (TCB-HFM) [18], simple hot box heat flux meter (SHB-HFM) [19], infrared thermography (IRT) method [20], and temperature-based method (TBM) [21]. An overview of the said experimental approaches introducing the procedures for estimating the U-value was provided in [22,23]. Figure 1 illustrates schematics of the aforementioned methods and the required codes used in the literature for the thermal parameter diagnosis of building envelopes [24]. In this figure, $S_{1,2,3}$ is the thickness of material layer in the component. $K_{1,2,3}$ is the thermal conductivity of material, R_{si} is the thermal resistance of internal surface, R_{se} is the thermal resistance of external surface, T_i is the interior temperature, T_e is the exterior temperature, T_{si} is the interior surface temperature, q_i is heat flow passing through the unit of area, h_i is the total internal heat transfer coefficient, and h_e is the total external heat transfer coefficient.
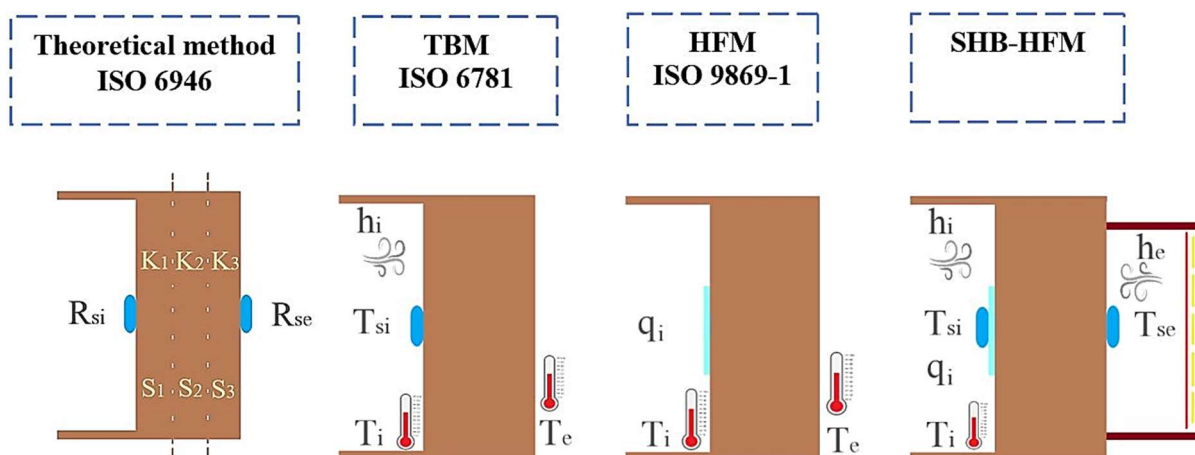
Figure 1. Schematic of the current techniques for thermal parameter diagnosis of the building envelops [24].

There are a variety of devices used to infer the thermal parameters of building models following the said methods [25]. One of the main problems in the application of the current systems is the high cost of measuring devices and sensor instrumentation. For instance, traditionally, in HFM method, the heat flux sensors are only installed on one side of the building envelopes. In fact, installing a heat flux meter on both sides of the building component can attenuate the monitoring error, massively [19]. However, due to the high cost of the required devices and the budget limitation, this application is not feasible in all building energy-monitoring projects [26]. Taking the advantage of temperature, humidity, and air velocity sensors, Esfandiari et al. determined the optimum set point of indoor temperature for a green building index office to improve sustainable energy policies for a tropical climate [27]. In terms of TBM, a combination of unintegrated commercial sensor devices has widely been used to estimate the energy performance of buildings. Kim et al. used T-type thermocouples and an H. Inc._4-ch data logger to measure the U-value, estimate the energy efficiency, and apply the retrofit to a house case study [28]. In fact, TESTO equipment is one of the most popular TBM monitoring systems in the market [29]. Various models of this monitoring system such as TESTO 635-2 and TESTO 635-4 [30], TESTO 435-1 [31] and TESTO 435-2 [32], have been used in the literature to characterize thermal properties of buildings. The instrumentation costs for a single measurement point using the TESTO systems could vary from EUR 570 to 1032, consequently, the thermal analysis of structures is limited to an inadequate number of measurement points.

Our literature review demonstrated an application of low-cost sensors as an alternative to traditional monitoring devices in building monitoring [33,34]. A systematic literature review on the application of low-cost sensors to monitor two aspects of structural and indoor parameters of buildings can be found in an article written by Mobaraki et al. [35]. Studies have also demonstrated the significance of the Internet of Things (IoT) to reduce cost, improve efficiency, and obtain data-oriented maintenance services. Aiming to improve the application of low-cost monitoring devices, the integration of low-cost sensors and IoT has been proposed in the literature [36]. Examples of these studies are in terms of monitoring indoor air quality [37], structural parameters of buildings [38], micro-climate of cultural heritage monuments [39], and also controlling the heating, ventilation, and air conditioning (HVAC) [40]. In addition, scholars have been seeking innovative Industry 4.0 solutions to monitor buildings by using smart devices and low-cost sensors, efficiently and economically [41]. Various applications of Industry 4.0 have been presented in the literature to carry out low-cost structural health monitoring [42], reduce both the energy and maintenance costs of buildings [43], and provide real-time monitoring and controlling of home appliances [44]. The growing interest in low-cost solutions for monitoring operations in different fields is illustrated in Figure 2, in which the number of publications in the Scopus

database have been ordered by years (from 2011 to 2021). In this figure, the publications have been clustered into the following engineering fields: civil and building, industrial, mechanical, architecture, medical and electronic.
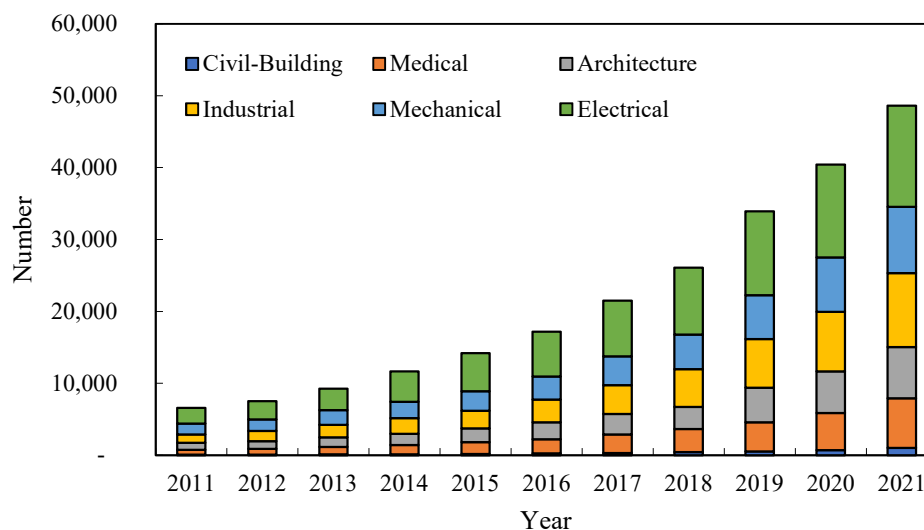

Figure 2. Number of works addressing low-cost sensors referenced in the Scopus database from 2011 to 2021 in different fields.

The analysis of Figure 2 showed that applications in civil and building engineering are scarce in comparison with other fields in the literature (such as electrical or mechanical engineering). For example, the number of publications in the civil and building engineering field in 2021 represented only 2.1% of the total studies published that year.

Aiming to deal with the high cost of traditional/commercial devices, various low-cost solutions have been proposed in the literature to determine the structural parameters of buildings [33], and also to derive the thermal parameters of building envelopes. Taking the advantage of low-cost sensors, Martin-Garin et al. developed a building environmental monitoring system. The authors conducted a comparative analysis of the obtained results, and developed a series of guidelines so as to select the most appropriate sensor for monitoring projects [45]. Ali et al. developed a low-cost open-source hardware and software platform to monitor the performance of buildings, called Elemental, that was designed to provide data on indoor environmental quality, energy usage, and other factors to users [46]. A group of authors developed a low-cost monitoring system and stationed it at the Mosque-Cathedral of Cordoba in Spain in order to assess the behavior of interior temperature and relative humidity in relation to exterior weather condition, public hours, and interior design [47]. A principal line of investigation in the field of energy efficiency focused on the enclosures of building facades. Echarri et al. studied the destructive thermal monitoring of a residential house using an inexpensive monitoring system [48]. To this aim, they opened the enclosure and positioned low-cost sensors of temperature, air velocity, and relative humidity in different layers of the enclosures, as well as the indoor and outdoor surfaces. The authors presented comparative results of temperature gradients versus a non-destructive monitoring system, providing the U-value. Marques et al. developed a cheap wireless measurement system to estimate the U-value of building envelopes [49]. Functionality of the proposed system followed the TESTO system in terms of number of measurement points associated with the indoor and outdoor temperatures, as well as the indoor surface one. This implied that their experiment was targeted at the three measurements of the wall surface temperature but only a single measurement of interior and exterior temperature. Serroni et al. presented a multi-sensor device, operating based on a thermal camera to provide the thermal maps of the indoor surface temperature [50]. In this study, the authors used a desk node and data of a weather station to determine the indoor and outdoor air temperature, respectively. In fact, the main limitation of this approach

was related to the low accuracy, up to 20%, due to the strong dependency of the thermal camera on environmental conditions. On the other hand, a combination of the commercial unintegrated sensor devices, such as T-type thermocouples and H. Inc._4-ch data logger, have been studied by Kim et al. to estimate the energy performance of buildings using TBM [28].

In the reviewed articles, different methodologies using unintegrated sensor devices (Kim et al. [28]) and low-cost sensors to characterize the thermal parameters of building envelopes have been studied. However, in the proposed low-cost solutions (Marquez et al. [49]), conducting thermal monitoring of buildings is limited to a small area, which could not be representative enough of the study's elements. This can be introduced by the uncertainties associated with the heterogeneity in the composition of walls. Moreover, thermal monitoring of buildings contains a high level of uncertainties associated with the utilized sensor devices (Serroni et al. [50]). All of the aforementioned factors influenced the precision of the data required for the estimation of the U-value. In fact, enhancing the number of measurement points using low-cost sensors not only enabled monitoring a sufficient area of building envelopes, but it also provided studying the statistical benefits of increasing the number of sensor/measurement points.

Aiming to address the aforementioned issues and fill these gaps in the literature, the main novelty of this study was to present a hyper-efficient Arduino transmittance-meter (HEAT) with a standardized Bluetooth communication protocol for saving and transmitting data. Unlike conventional TBM U-value metering devices, a HEAT was based on multiple measurements of the three main parameters required to estimate the U-value: the indoor and outdoor temperature of a building and the temperature of the inner surface of the wall. A HEAT is capable of recording as much data as engineers require to estimate a U-value. It is also scalable, meaning that it can be used for thermal monitoring of all sizes of real-scale structures, and also for a temperature-controlled box model. A HEAT is also low-cost because its development is based entirely on low-cost devices. To develop an accurate transmittance meter, a HEAT was used with three low-cost temperature sensors (MLX90604 [51], MAX30205 [52], and DS18B20 [53]) (manufacturer, address of manufacturer) to monitor the surface temperature of building envelopes. To check the applicability of a HEAT, an experimental study carried out for thermal monitoring of a temperature-controlled box model, and the outputs of the three HEATs (MLX90604, MAX30205, and DS18B20) were compared with those captured by a known commercial U-value meter, TESTO 435-1.

This study is organized as follows. Section 2 presents the available codes and empirical formulas required for the thermal diagnosis of buildings using the TBM. Section 3 provides a comprehensive explanation of established HEATs, including the characteristics of the utilized hardware and quantities of the installed low-cost sensors. In Section 4, a description of the experiment as well as sensitivity analysis of the infrared sensors are given. Then, in Section 5, the measurement results are analyzed and discussed as part of the comparison with the outputs of the TESTO 435-1. Finally, the conclusions of this study are presented in Section 6.

2. Measurement Methodology

Multiple standards define a set of instructions for estimating the thermal parameters of building elements. These standards include multiple provisions, such as test duration, frequency of observations, seasonality of experiments, treatment of outliers, and methods of verifying observations [54]. Some of the most common standards are presented here. ISO 6946:2017, which is for theoretical calculation of building U-values, considers the thicknesses of materials used to build a wall and provides the air heat transfer coefficient to be used in the TBM [55]. ISO 9869:2014, which uses the HFM method to calculate the thermal transmittance of building components under steady-state conditions, based on the assumption that average values of heat flow rate and temperatures over a reasonably long period of time (minimum 72 h) gives an estimate of the steady-state condition [56]. ISO

6781-3:2015 assesses building performance in terms of heat, air, and moisture using infrared methods [57]. ISO 10456:2007 presents methods for calculating the thermal parameters of buildings by introducing the thermal conductivity of different materials [58].

Determining the transmittance parameter of the building envelopes is costly and time-consuming in terms of various aspects including test duration, number of parameter measurements required, weather conditions (cloudy vs. sunny), and magnitude of temperature difference. A TBM would be suitable for overcoming these limitations, considering the parameters required to obtain the transmittance parameter via the methodologies available in the literature (as described in Section 1). The TBM is a non-destructive average technique that determines the U-value of building envelopes by measuring and substituting the interior temperature (T_i), exterior temperature (T_e), and the interior surface temperature of an object (T_{si}), as shown in Equation (1). This technique is based on Newton's law of cooling, which states that the rate of heat transfer is proportional to the difference in temperature between a body and its surroundings. Equation (1) was derived from Equation (2), which is used for the HFM method (as per ISO 9869:2014 requirements). Thus, the only difference between these two methods is that in the TBM, it is not necessary to consider the effect of heat flux through the object, while it is necessary in the HFM method. In Equations (1) and (2), n is the number of measurements, U is the transmittance parameter (W/m^2·K), T_i is the interior temperature at instant j (°C), T_e is the exterior temperature (°C), T_{si} is the interior surface temperature (°C), q is heat flow passing through the unit of area (W/m^2), and h_{ci} is the total internal heat transfer coefficient, which is equal to 7.69 W/m^2·K, and can be derived from ISO 6949: 2017.

$$U = \frac{\sum_{j=1}^{n}\left(T_{i(j)} - T_{si(j)}\right)}{\sum_{j=1}^{n}\left(T_{i(j)} - T_{e(j)}\right)} h_{ci} \tag{1}$$

$$U = \frac{\sum_{j=1}^{n} q_j}{\sum_{j=1}^{n}\left(T_{i(j)} - T_{e(j)}\right)} \tag{2}$$

3. Establishing a Hyper-Efficient Arduino Transmittance-Meter (HEAT)

This section presents a comprehensive explanation of the hardware utilized for the development of three HEATs, the measurement and calculation methodologies for estimation of U-value, and the techniques proposed for increasing HEAT accuracy.

3.1. Hardware

There are various types of low-cost temperature sensors available in the market to measure the ambient temperature and surface temperature of an object through contact and contactless infrared methods. Table 2 lists the most common sensors available, including basic information such as model, application, detection range, accuracy, cost, and associated references in the literature. The differences between these alternatives are mainly in terms of the price and characteristics presented in the associated catalog. These characteristics are as follows: (1) detection range: the detection range indicates the lowest and highest temperature that can be measured by the sensor; (2) accuracy: this parameter introduces how close the measured temperature is to the real one; (3) resolution: this characteristic refers to the capability of the sensor to show the smallest changes of temperature; (4) response time: this is for addressing the time needed by the sensor to measure a change of temperature; (5) communication protocol (e.g., with microcontrollers): depending on the monitoring project, this factor plays an important role in the selection of the low-cost sensors. The most common alternative is the inter-integrated circuit communication (I^{2}C) protocol which requires only two wires for the synchronized communication of 64 low-cost sensors to an Arduino microcontroller. It also must be mentioned that I^{2}C is less susceptible to noise than single wire/bus serial peripheral interface (SPI) communication protocols. More information about the main characteristics of the sensors can be found in [59,60].

Table 2. List of the common contact, contactless, and infrared temperature low-cost sensors in the market.

Model	Operation	Application	Detection Range (°C)	Accuracy (°C)	Cost (EUR)	Ref.
NTC	Contact	Environmental and structural fitness	(−55 to 200)	1	1	[61]
DS18B20			(−55 to 125)	0.5	4.9	[62]
MAX30205			(0 to 70)	0.1	12.9	[63]
TMP006	Infrared	Environmental and structural Medical	(−40 to 125)	1	6	[64]
MLX90614			(−40 to 125)	0.5	29.6	[65]
DHT11	Contactless	Environmental	(0 to 50)	2	1.56	[66]
DHT22			(−40 to 80)	0.5	5.40	[67]
SHT10			(−40 to 125)	0.5	4.57	[68]
SHT21			(−40 to 125)	0.3	4.61	[45]
SHT35			(−40 to 125)	0.2	5.76	[69]
BMP180			(−40 to 85)	2	3.72	[70]
BMP280			(−40 to 85)	1	3.59	[71]
LM35			(−55 to 125)	1	2.80	[72]

Among the low-cost sensors listed in Table 2, two contact-based low-cost sensors (MAX30205 and DS18B20) and one infrared model (MLX90614) were selected to develop the three HEATs. The selected sensors have various specifications regarding their application (environmental/structural monitoring, medical, and fitness issues), functionality (contact-based, infrared, and contactless sensors), accuracy (0.2 °C to 0.5 °C), cost (EUR 4.95 to EUR 29.6), and detection range (−55 °C to 125 °C). It is worth noting the use of infrared sensors in this study attenuates the difficulties of the project in terms of the sensors' attachment to the study's elements. In addition, it provides to investigating the possibility of reducing the uncertainties associated with the use of contact sensors for detecting the surface temperature of the object. Among the two infrared sensors (TNP006 [73] and MLX90614) presented in Table 2, MLX90614 was chosen due to its higher accuracy. It also must be mentioned that, among the chosen three sensors, MLX90614, comes fully factory calibrated. SHT35 was calibrated by the authors using statistical reference obtained by averaging the measurements of 30 SHT35 sensors [74]. However, the DS18B20 sensor, as well as MAX30205, were uncalibrated. In fact, this disparate specification of the chosen sensors provided the opportunity to compare and study the statistical benefits of increasing the number of calibrated and uncalibrated sensors, under the same conditions.

Each HEAT operates independently, as it captures the surface temperature of the temperature-controlled box model separately using each of the sensors (MAX30205, DS18B20, and MLX90604). All three HEATs were built into individual Arduino MEGA microcontrollers. Eight copies of each of the aforementioned sensors measured the surface temperature of the object for each individual HEAT (HEAT MAX30205, HEAT DS18B20, and HEAT MLX90614). The indoor temperature was measured by the eight duplicated MLX90604 infrared sensors as this sensor can measure both surface and environmental temperatures. In addition, eight duplicated SHT35 sensors were used to measure the exterior temperature. To save the measurements, a wireless Bluetooth communication protocol was employed (using HC-05 low-cost sensor) between the HEATs and the laptop. This implies that each individual HEAT was connected to the laptop through a virtual communication port and transferred its measurements, separately.

3.2. The Developed HEATs

Each HEAT contains (1) an Arduino microcontroller (MEGA 2560) [75], a small-sized (10.16 cm × 5.34 cm) computer considered to be the brain of the three HEATs and which receives and applies the instructions required for experiments [76]; (2) a TCA9548A multiplexer to enhance the amount of data that can be transmitted over the developed sensor network (except for the HEAT DS18B20) [77]; (3) a breadboard to facilitate the connections

between different parts of the HEATs; (4) a DS3231 clock sensor to define and save the exact measurement times [78]; (5) a HC-05 low-cost Bluetooth sensor to transfer the readings from the HEATs to the laptop, and (6) the explained low-cost temperature sensors.

The indoor modules of the HEAT MLX90604, HEAT DS18B20, HEAT MAX30205, and outdoor module of them are shown in Figures 3a, 4a, 5a and 6a, respectively. The wiring of the Fritzing software modules are depicted in Figure 3b (HEAT MLX90604), Figure 4b (HEAT DS18B20), Figure 5b (HEAT MAX30205), and Figure 6b (outdoor module).
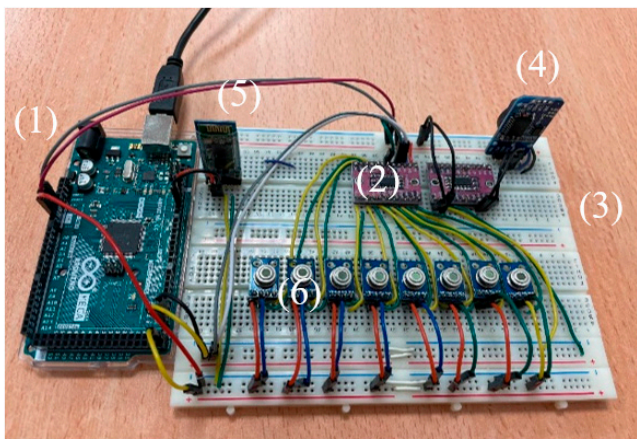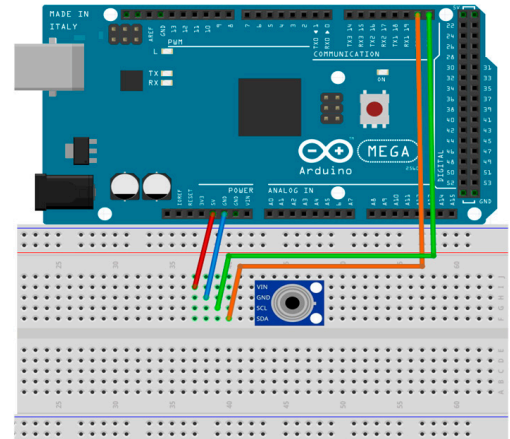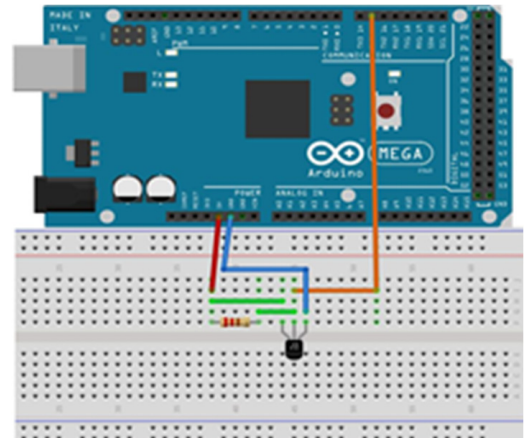

(**a**)   (**b**)

Figure 3. HEAT MLX90614: (**a**) Indoor module and wire connections of one MLX90614 sensor with the Arduino Mega (**b**).
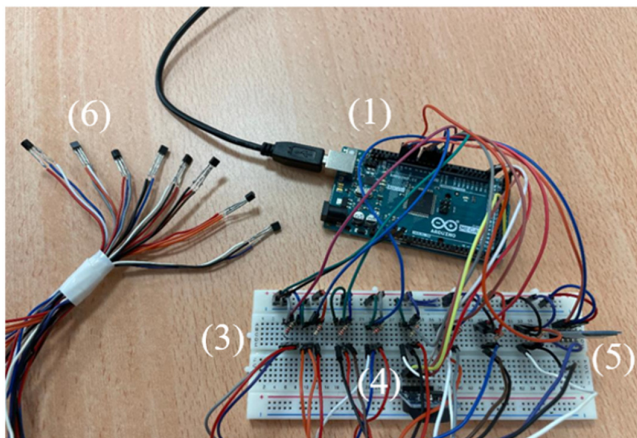
(**a**)   (**b**)

Figure 4. HEAT DS18B20: (**a**) Indoor module and wire connections of one DS18B20 sensor with the Arduino Mega (**b**).
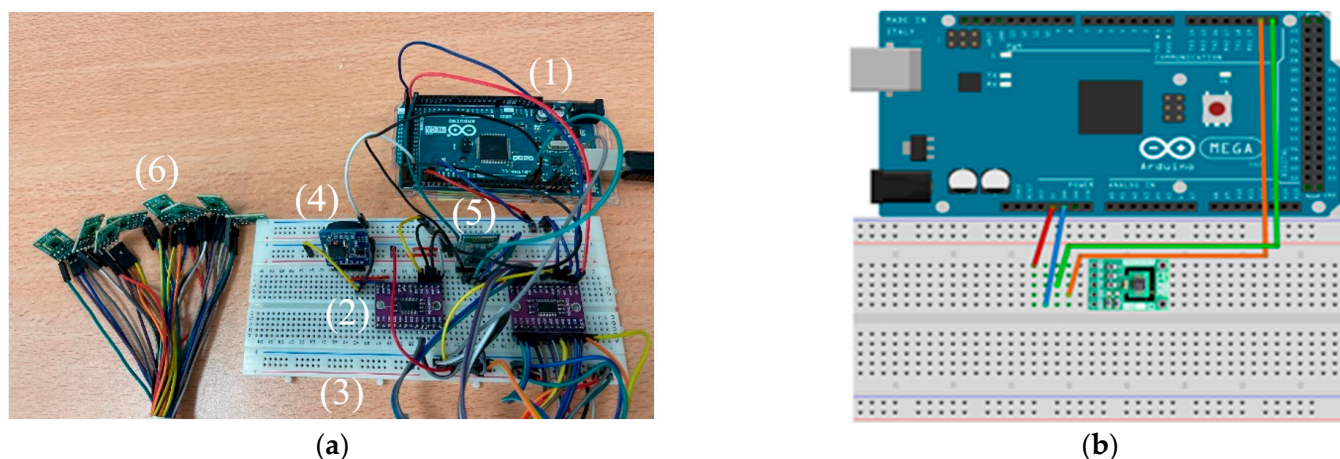
Figure 5. HEAT MAX30205: (**a**) Indoor module and wire connections of one MAX30205 sensor with the Arduino Mega (**b**).
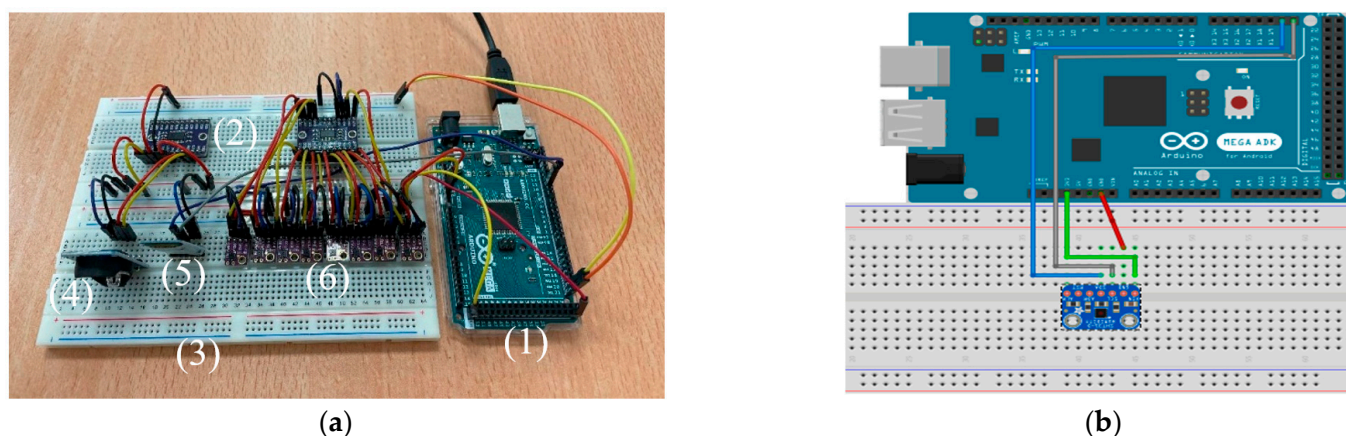

Figure 6. Outdoor module of HEAT (**a**) and wire connections of one SHT35 sensor with the Arduino Mega (**b**).

3.3. Measurement Methodology and Developed Algorithm

A two-phase algorithm was developed in MATLAB (version, manufacture, city, state abbreviation, country) to determine the U-value of the temperature-controlled box model [79]. In the first phase, the U-value is estimated based on the average measurements of each of the three parameters (T_i, T_e, and T_{si}) corresponding to an individual HEAT. Then, the U-values calculated by each HEAT are compared with those derived from the TESTO 435-1. In the second phase, two different approaches are introduced to increase the accuracy of the associated HEAT in Phase 1. These approaches include estimating the U-value (1) based on the median value of the parameter measurements and (2) after omitting the outliers of the measurements. In each phase, the accuracies of the HEATs were checked using the TESTO 4535-1 measurements.

A step-by-step explanation of the two phases and the three approaches cited are as follows:

Phase 1:

- Receive the HEAT observations via the wireless Bluetooth protocol.
- Calculate the mean value of the measurements of the eight sensors associated with interior temperature (T_i), exterior temperature (T_e), and interior surface temperature (T_{si}).

-   Substitute the mean values of the parameters into Equation (1), determine the U-value of each HEAT, and then calculate the difference between the obtained results and those derived from the TESTO 435-1.

    Phase 2:

-   *Approach 1*
    -   Specify the outliers (measurements that fall below and above the 5th and 95th percentiles) and remove them from the observations.
    -   Substitute the mean values of the parameters into Equation (1), determine the U-value, and then calculate the difference between the obtained results and those derived from the TESTO 435-1.

-   *Approach 2*
    -   Define the median values of the eight measurements associated with the observations of each of the three parameters (T_i, T_e, and T_{si}).
    -   Substitute the median values of the parameters into Equation (1), determine the U-value, and then calculate the difference between the obtained results and those derived from the TESTO 435-1.

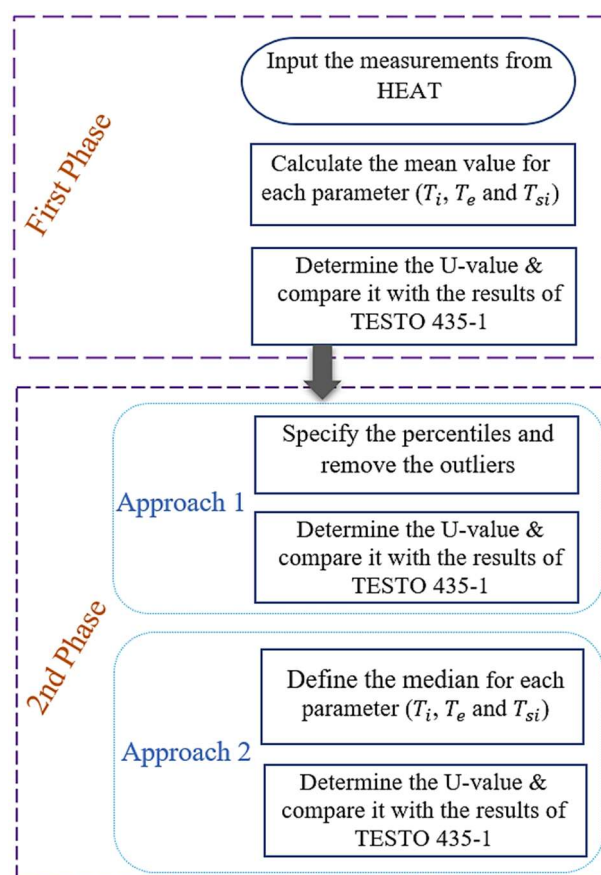Figure 7 shows a summary of the steps performed to assess the HEAT operation.

Figure 7. Algorithm to infer the U-value from the measurements of HEAT and the defined approaches to increase the precision of monitoring.

4. Laboratory Testing

This section describes the experimental campaign designed to prove the applicability of the established HEATs. To do so, detailed explanations of the temperature-controlled box model, test condition, and sensitivity of the infrared MLX90604 sensors are provided.

4.1. Description of the Test

The temperature-controlled box model was purchased by the Civil Engineering Department of the University of Castilla-La Mancha (UCLM) in Ciudad Real, Spain, to determine the applicability of the three HEATs. This temperature-controlled box model was 40 cm × 40 cm × 40 cm and had a substitutable side wall utilized to diagnose the thermal parameter of different types of wall materials, typical glass, and two-layer windows. For this diagnosis, the indoor and outdoor temperatures of the box model and the interior surface temperature were captured at fixed indoor and outdoor temperatures to represent steady-state conditions. A 9-layer 25 cm × 25 cm × 2 cm piece of plywood was considered as the wall, because a plywood wall would ensure that the temperature difference between the layers would be the result of each layer-specific thermal transmittance value. The two sets of contact sensors (eight kits in each) and the three TESTO thermometers were then attached to the wall model using thermally conductive adhesive tape. These sensors were attached to different parts of the wall to allow the actual wall temperature to be determined, and they were located at a distance of 17 cm, far from the heat source. Regarding the contactless infrared sensors, they were located at a distance of 12.5 cm, far from the heat source. As heat is gained and lost in different parts of the house model, the roof and three other walls were isolated with polystyrene board 5 cm and 2 cm thick, respectively. Four holes were made in the corners of the model to insert sensor set cables to measure the indoor and inside surface temperatures, after which, the holes were covered with high-quality cotton. A 40 W incandescent lamp with a covering steel cap was used as a heat source. The temperature sensor of the thermostat was placed on top of the cap of the heat source and was connected to the thermostat. This implies that one could fix the indoor temperature by adjusting the thermostat to the required level. Figure 8 shows the temperature-controlled box model, revealing the different elements of the temperature-controlled box model, attached sensors, and the TESTO 435-1.
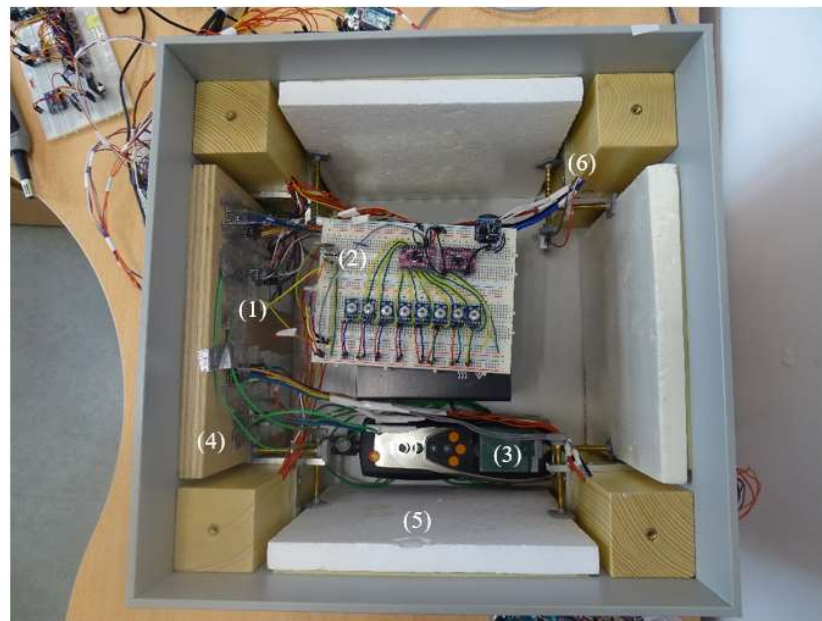

Figure 8. Installation of the contact DS18B20/MAX30205: sensors (1), infrared sensor MLX90614 (2), indoor module of TESTO 435-1 (3) and different elements of the temperature-controlled box model: plywood wall (4), polystyrene (5), corner hole (6).

The experiment was conducted in a controlled environment in one of the offices of the UCLM. During the test, the temperature of the office (the exterior temperature of the house model) was controlled and adjusted via air conditioning. The indoor and outdoor temperatures of the model were fixed at 40 °C and 25 °C, respectively, providing a

minimum difference of 10 °C to 15 °C. Obtaining such a difference was achieved by turning on the heat source of the box model (a 40 W incandescent lamp) and also the air conditioner, from a day prior to initiating the experiment. In essence, carrying out the real-time indoor and outdoor temperature monitoring of the box model using the Bluetooth communication protocol, before and during the experiment, provided the authors to take control of the steady-state condition. The following conditions were considered during the test as per ISO 6781 and ISO 9869:

-   The achievement of a steady-state condition.
-   The outdoor temperature did not exceed ± 10 °C 24 h prior to the experiment.
-   The indoor and outdoor temperatures were not altered by more than ± 2 °C and ± 5 °C, respectively, with respect to their initial values during the experiment.
-   Direct solar radiation was kept off the temperature-controlled box model during the test.

The experiment was conducted continuously for 17 h, during which, the HEATs were adjusted at a sampling frequency of 5 min. In total, more than 200 measurements of the three parameters were obtained for each set. Figure 9 shows the configuration of the experiments, including the introduction of different elements.
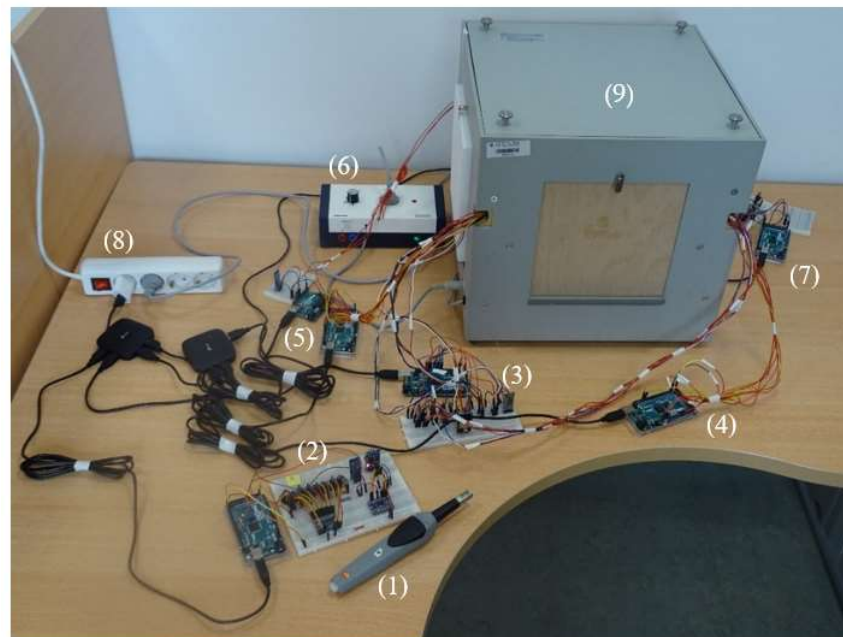

Figure 9. The developed sensors and test condition: (1) outdoor probe of TESTO 435-1 (T_e), (2) outdoor module sensor SHT35 (T_e), (3) sensor DS18B20, (4) sensor MLX90614, (5) sensors for controlling the indoor/outdoor temperature, (6) thermostat, (7) sensor MAX30205, (8) power source, and (9) the temperature-controlled box model.

4.2. Sensitivity of the Infrared Sensor

The infrared MLX90614 sensor detected the surface temperature of an object from a distance of 3 to 6 cm. To obtain the highest measurement accuracy from this sensor, a sensitivity analysis was performed to determine the optimal distance that it should be kept from an object. A preliminary test was performed using four distances (3 cm, 4 cm, 5 cm, and 6 cm) between the eight sensors and the plywood wall in the temperature-controlled box model. The average measurements obtained from the eight MLX90614 sensors were compared with those from the TESTO 435-1. As shown in Figure 10, the lowest difference range was obtained at a distance of 3 cm from the object. As expected, an increase in the distance attenuated the precision of the sensors as higher difference ranges occurred at

distances of 4 cm, 5 cm, and 6 cm. Therefore, in the test, the MLX90614 sensors were placed 3 cm from the wall of the temperature-controlled box model.
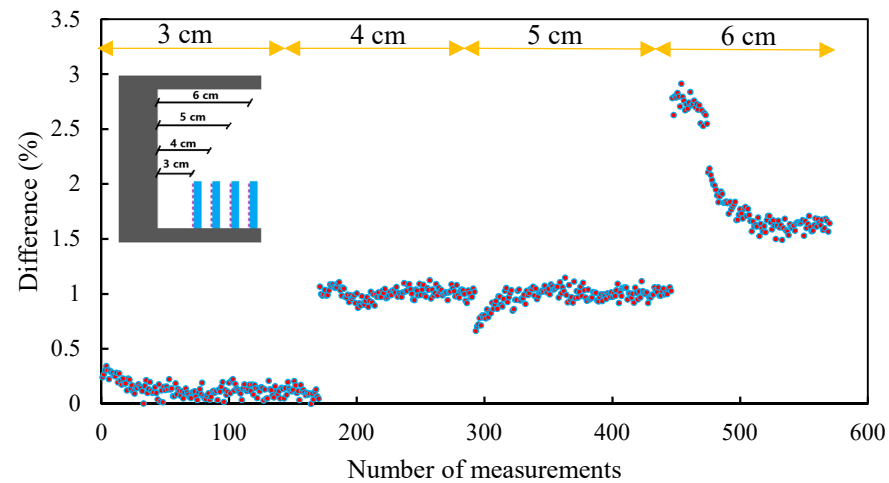

Figure 10. Sensitivity analysis of the HEAT MLX90614.

5. Results and Discussion

By applying Phase 1 of the algorithm proposed in Section 3.3, the T_i, T_e, and T_{si} were measured for the three HEATs and the mean value of each parameter was calculated. Figure 11 shows the comparison of the average surface measurements ($T_{si} = (T_{si1} + T_{si2} + T_{si3} + \ldots + T_{si8})/8$) derived from the MLX90604, MAX30205, and DS18B20 HEATs with those derived from the TESTO 435-1 ($T_{si} = (T_{si1} + T_{si2} + T_{si3})/3$). The test was considered successful when steady-state conditions were achieved and variations in temperature did not exceed more than 1.3 °C for any of the three HEATs and TESTO 435-1. Overall, the surface temperature measurements generated by the MLX90604 HEAT were the most similar to those of the TESTO 435-1.
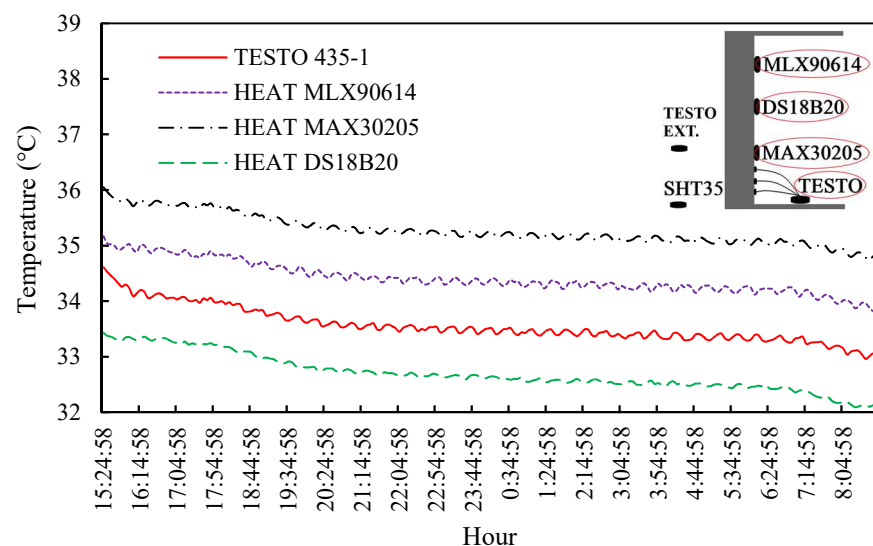

Figure 11. Evolution of the surface temperatures recorded by the three HEATs and the one captured by TESTO 435-1.

To better understand the discrepancies in the measurements, the standard deviations (SDs) of the wall surface temperatures recorded by the HEATs are shown in Figure 12, wherein the horizontal axis shows the number of measurements during the monitoring period and the vertical axis shows the SD range. Among the HEATs, the MAX3020 had

the lowest SD range of $0.52 \leq SD_{MAX30205} \leq 0.69$. However, the SDs of the three HEATs increased during steady-state conditions. According to the experiences of the authors, the low-cost sensors performed better in dynamic situations than static ones.
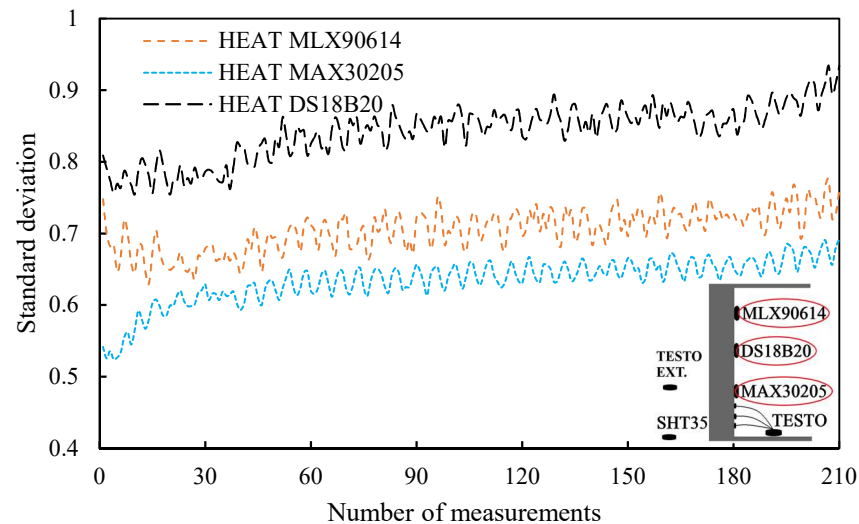

Figure 12. Standard deviations of the surface temperature measurements captured by sensors of the HEAT MAX3020, HEAT DS18B20, and HEAT MLX90614.

To show the significance of increasing the number of sensors in monitoring projects, Figure 13 illustrates the distances between the measurements of a single DS18B20 sensor with the associated average value of the eight sensors and with that obtained from the TESTO 435-1. For simplicity, only the measurements from DS18B20 HEAT are presented. As expected, the accuracy of monitoring improved with the increase in the number of sensors. This improvement in monitoring quality was demonstrated by a 54% difference reduction when the number of measurements increased from one to eight.
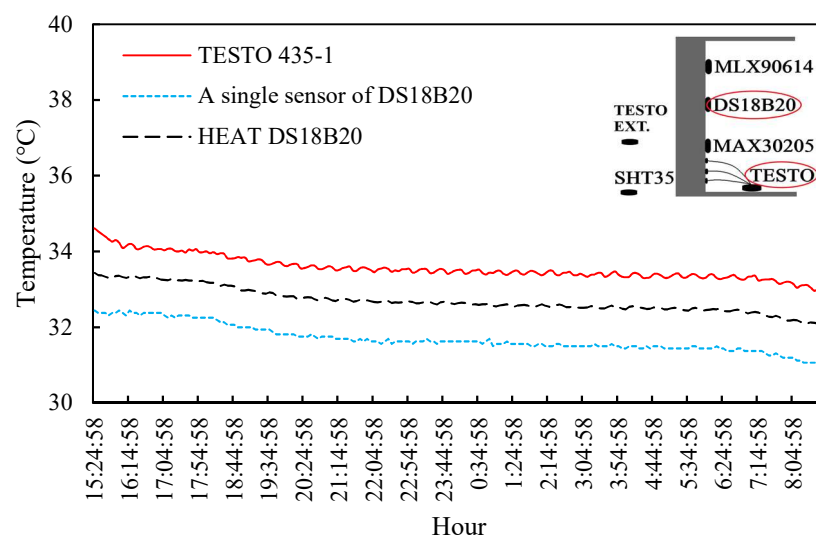

Figure 13. Comparison between indoor temperature measurements of TESTO 435-1 and that of a single sensor of DS18B20, and the associated average of the 8 sensors of DS18B20.

Figure 14 shows the accuracy of the three HEATs based on their T_{si} and U-value measurements (left-hand vertical axis), and the cost efficiency of each individual HEAT (right-hand vertical axis). Overall, the range of difference for the HEAT T_{si} measurements was not considerable; however, a high difference range was observed for the U-values obtained. For example, the MAX30205 HEAT returned a 5.1% difference for T_{si} but an

average difference of -22.8% for the associated U-value. This is consistent with the interactions between errors from different sensors (for T_i, T_e, and T_{si} measurements) and the combination of various factors used to estimate the U-value. In fact, the differences were within an acceptable range for the measurements from the MLX90604 HEAT, as a TBM transmittance-meter [21]. In terms of the T_{si} and U-value measurements, the differences obtained from this HEAT were 2.5% and -8.60%, respectively. Further analysis of Figure 14 shows that the ranges of difference obtained for the MLX90614 and MAX30205 HEATs were negative. This is because the values calculated for the transmittance parameters were higher than those of the TESTO 435-1. The MLX90614 HEAT not only had an acceptable difference range but also had a favorable cost, demonstrating a 63.2% cost reduction, as compared with the TESTO 435-1. Meanwhile, the ranges of the cost reduction for the MAX30205 and DS18B20 HEATs were 76.2% and 82.4%, respectively. Table 3 summarizes the commercial full instrumentation costs for all three HEATs.
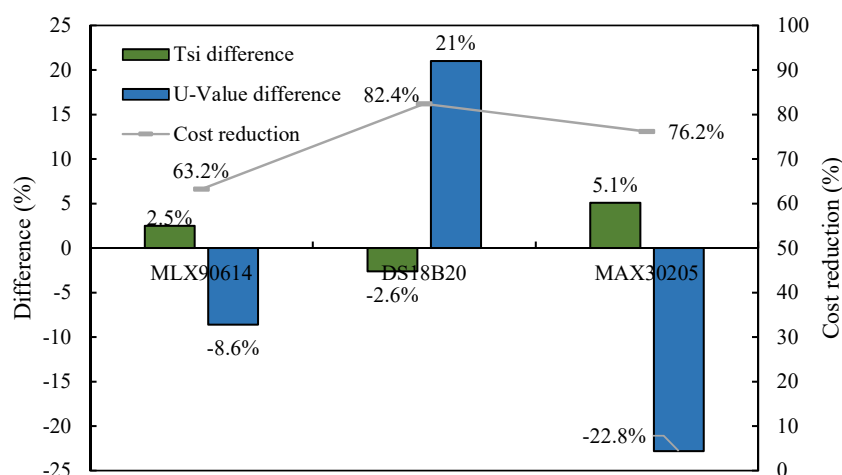

Figure 14. Cost reduction of the developed sensor compared with TESTO, as well as the differences of the individual kits and three HEATs.

Table 3. Cost comparison between the three developed sensors with the commercial TESTO thermometers.

	HEAT MLX90614		HEAT MAX30205		HEAT DS18B20		TESTO 435-1
Components	Price (EUR)	Number	Price (EUR)	Number	Price (EUR)	Number	
Sensors	29.6	8	12.9	8	4.95	8	
Breadboard	3.5	1	3.5	1	3.5	1	
Arduino	35.5	1	35.5	1	35.5	1	
Multiplexer	1.2	2	1.2	2	-	-	
Clock sensor	1.3	1	1.3	1	1.3	1	
Bluetooth sensor	4.5	1	4.5	1	4.5	1	
Resistor	-	-	-	-	0.2	8	
SHT35 set (T_e)	92	1	92	1	92	1	
Total Cost (EUR)	380		246		181		1032

The cost comparison summarized in Table 3 is based on the price of the different pieces of hardware used to install each HEAT, including common elements such as the breadboard, Arduino, clock, and Bluetooth sensors, and outdoor module of the SHT35 set (to calculate T_e). In addition, an individual MLX90614 and MAX30205 HEATs contain a multiplexer for I2C communication between the kits. However, DS18B20 HEAT contains a resistor required to install the kit. In this table, the assembling and programming cost of the HEATs are not accounted for in this comparison. Overall, the total costs calculated for the indoor and outdoor HEAT modules are EUR 181 for the DS18B20, EUR 246 for MAX30205, and

EUR 380 for MLX90614. The results show that the MLX90604 HEAT achieved the highest accuracy and was the most expensive. However, it saved up to 63.2% of the monitoring cost of the TESTO 435-1 (Figure 14). Furthermore, owing to the high cost of standard devices in the market, providing spatial measurements for the required parameters were almost infeasible for the other methodologies, and not everyone can afford them for their projects. This highlights the efficiency of the MLX90614 HEAT, which can provide engineers with an inexpensive way to conduct high-density thermal monitoring of building envelopes.

Figure 15 compares the measurements from the TESTO 435-1 and MLX90614 HEAT in terms of the U-value, including all the parameters required for calculation. The results show that, during the 17 h of monitoring, there were limited variations in the T_i, T_e, and T_{si} measurements as recorded by the MLX90614 HEAT. These variations included a T_i value ranging from 39.6 °C to 41.0 °C (a difference of 0.4 °C), a T_e value that fluctuated between 22.7 °C and 24.9 °C (a difference of 2.2 °C), and a T_{si} value for the wall that varied between 33.8 °C and 35.2 °C (a difference of 1.4 °C). These measurements resulted in an average U-value of 2.62 W/m²·K for the wooden panel in the temperature-controlled box model.
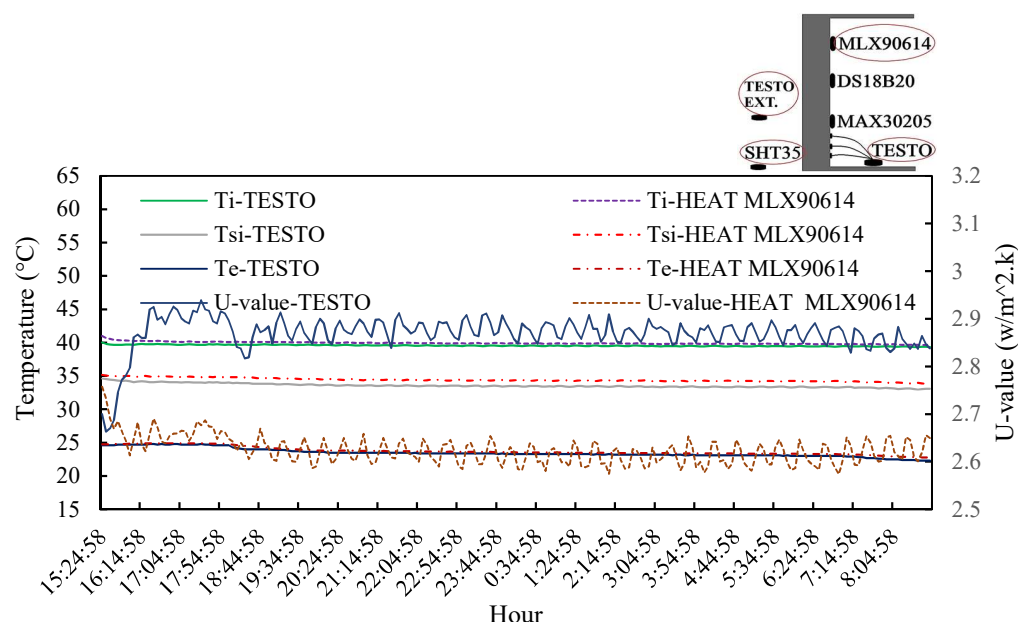

Figure 15. Comparison between the results of the HEAT MLX90614 and TESTO 435-1 in terms of T_i, T_e, T_{si}, and the U-value.

Figure 15 also shows the slight difference between the measurements of the MLX90614 HEAT and TESTO 435-1. The difference between the average exterior temperature measured with the MLX90614 HEAT (23.7 °C) and the TESTO 435-1 (23.5 °C) is, in particular, only 0.2 °C; this is a negligible difference (only 0.85% higher than the measurement of TESTO 435-1). In addition, the average indoor temperature measurements taken by the MLX90614 HEAT (39.6 ≪ T_i(°C) ≪ 41.0) are only 0.9% higher than those of the TESTO 435-1 (39.3 ≪ T_i(°C) ≪ 40.0).

In Phase 2 of the algorithm, two approaches were implemented to increase the accuracy of the MLX90614 HEAT. As mentioned in Section 3.3, the first approach was based on detecting outliers. In general, sensor errors can be categorized as soft (e.g., bias and environmental noises) and hard (physical damage to the sensors during a test). Thus, it is vital to determine the potential effect of soft and hard errors, and consider them in the final assessment of sensors. Outliers are measurements that lie an abnormal distance from the greatest number of measurements; observations that fall above and below the 95th and 5th percentiles, in particular, are considered outliers. In this study, detecting the outliers and removing them from the measurement data caused the error of the MLX90604 HEAT be decreased from 8.6% to 7.7% (a decrease of 11.6%).

Meanwhile, following the second approach, the U-value was calculated by specifying the median value of the eight sensors associated with the three parameter measurements. In this scenario, the error of the MLX90604 HEAT was reduced from 8.6% to 7.2% (a decrease of 19.4%). These results indicate that using the median hypothesis can improve the estimation of the U-value more than using the mean value or eliminating the outliers. This event can be explained as follows: (1) while the mean value and SD are statistically sensitive to outliers, the median is an impractical statistical measurement as it is at risk from outliers lower than the mean value and (2) the demand for outlier detection is increased when the same kind of measurements are received from several sources of information. In this experiment, an individual parameter was measured using only eight sensors at a single time, which is not too many sensors.

6. Conclusions

In this article, a methodology to improve thermal monitoring of buildings was proposed by using a new transmittance-meter. The novelty of this low-cost monitoring system, HEAT, is to provide the user with the statistical benefits of increasing the number of measurement points which attenuates the uncertainties of U-value estimation. On the basis of TBM, a HEAT operates based on eight measurements of the principal parameters needed to estimate the U-value. To prove the significance of the proposed methodology, a HEAT was tested on three types of sensors, with diverse operations and accuracies. Aiming to validate the performance of a HEAT, simultaneous thermal monitoring of a temperature-controlled box model was carried out using the three HEATs and a common commercial transmittance-meter in the market, TESTO 435-1. Comparison of the results proved application of the proposed methodology, as evidenced by a high reduction of differences in terms of the surface temperature detection when the number of measurement points was increased from one to eight. Moreover, according to the proven cost-efficiency of a HEAT, when a number of measurement points were required for the in situ estimation of the U-value, a HEAT was utilized to carry out high-density thermal monitoring of building envelopes with a standard wireless communication protocol to transmit and save data. The authors recognize that the descriptions described in this article are a first step in the development of a HEAT, with the goal of utilizing it in building thermal monitoring applications. Indeed, the acquired results from the first version of a HEAT proved its efficiency and gave us encouragement to upgrade it for further applications. Future studies should address the use of the Internet as a principal communication protocol to deliver an IoT version of a HEAT, which enables real-time post-processing of the data and outlier detection. In addition, real application of a HEAT must be conducted for real-time updating of building information modeling which provides monitoring of thermal performance, before and after retrofitting of buildings.

Conflicts of Interest: The authors declare no conflict of interest.

References

1. Pi, Z.X.; Li, X.H.; Ding, Y.M.; Zhao, M.; Liu, Z.X. Demand Response Scheduling Algorithm of the Economic Energy Consumption in Buildings for Considering Comfortable Working Time and User Target Price. *Energy Build.* **2021**, *250*, 111252. [CrossRef]
2. Agency, A.E. Energy Data of Andalusia; Andalusian Energy Agency: Seville, Spain. Available online: https://www.eneragen.org/en/members/andalusian-energy-agency/ (accessed on 1 February 2022).
3. AIGUASOL. Barcelona Energy Improvement Plan (PMEB) and Barcelona Energy, Climate Change and Air Quality Plan (PECQ). Available online: https://aiguasol.coop/project/barcelona-energy-improvement-plan-energy-climate-change-air-quality-plan/ (accessed on 1 February 2022).
4. Wagiman, K.R.; Abdullah, M.N.; Hassan, M.Y.; Mohammad Radzi, N.H. A New Metric for Optimal Visual Comfort and Energy Efficiency of Building Lighting System Considering Daylight Using Multi-Objective Particle Swarm Optimization. *J. Build. Eng.* **2021**, *43*, 102525. [CrossRef]
5. Verbruggen, S.; Delghust, M.; Laverge, J.; JanssensArnold. Evaluation of the Relationship between Window Use and Physical Environmental Variables: Consistency, Seasonality and Diversity. *J. Build. Perform. Simul.* **2021**, *14*, 366–382. [CrossRef]
6. Susorova, I.; Stephens, B.; Skelton, B. The Effect of Balcony Thermal Breaks on Building Thermal and Energy Performance: Field Experiments and Energy Simulations in Chicago, IL. *Buildings* **2019**, *9*, 190. [CrossRef]
7. Roppel, P.; Lawton, M.; Norris, N. Thermal Performance of Building Envelope Details for Mid- and High-Rise Buildings. *ASHRAE Trans.* **2012**, *118*, 569–584.
8. Li, T.; Xia, J.; Chin, C.S.; Song, P. Investigation of the Thermal Performance of Lightweight Assembled Exterior Wall Panel (LAEWP) with Stud Connections. *Buildings* **2022**, *12*, 473. [CrossRef]
9. Currie, J.; Bros Williamson, J.; Stinson, J. Monitoring Thermal Upgrades to Ten Traditional Properties. *Hist. Scotl. Tech. Pap.* **2013**, *19*, 51. [CrossRef]
10. Biler, A.; Tavil, A.U.; Su, Y.; Khan, N. A Review of Performance Specifications and Studies of Trickle Vents. *Buildings* **2018**, *8*, 152. [CrossRef]
11. Ian, C.-S. Proposed Method for Measuring the Thermal Properties of Windows in the New BRANZ Guarded Hotbox. In Proceedings of the IPENZ Annual Conference 1997, Proceedings of: Engineering Our Nation's Future, Wellington, New Zealand, 7–10 February 1997; pp. 95–102.
12. Fang, Y.; Eames, P.C.; Norton, B.; Hyde, T.J. Experimental Validation of a Numerical Model for Heat Transfer in Vacuum Glazing. *Sol. Energy* **2006**, *80*, 564–577. [CrossRef]
13. Buratti, C.; Barelli, L.; Moretti, E. Application of Artificial Neural Network to Predict Thermal Transmittance of Wooden Windows. *Appl. Energy* **2012**, *98*, 425–432. [CrossRef]
14. Smith, N.; Isaacs, N.; Burgess, J.; Cox-Smith, I. Thermal Performance of Secondary Glazing as a Retrofit Alternative for Single-Glazed Windows. *Energy Build.* **2012**, *54*, 47–51. [CrossRef]
15. Lechowska, A.; Schnotale, J.; Fedorczak-Cisak, M.; Paszkowski, M. Measurement of thermal transmittance of multi-layer glazing with ultrathin internal glass partitions. *Czas. Tech.* **2014**, *2014*, 273–279.
16. Malvoni, M.; Baglivo, C.; Congedo, P.M.; Laforgia, D. CFD Modeling to Evaluate the Thermal Performances of Window Frames in Accordance with the ISO 10077. *Energy* **2016**, *111*, 430–438. [CrossRef]
17. Mellado Mascaraque, M.Á.; Castilla Pacual, F.J.; Oteiza, I.; Aparicio Secanellas, S. Hygrothermal Assessment of a Traditional Earthen Wall in a Dry Mediterranean Climate. *Build. Res. Inf.* **2020**, *48*, 632–644. [CrossRef]
18. Zhu, X.F.; Li, L.P.; Yin, X.B. An In-Situ Test Apparatus of Heat Transfer Coefficient for Building Envelope. *Build. Energy Effic.* **2012**, *256*, 57–60.
19. Meng, X.; Gao, Y.; Wang, Y.; Yan, B.; Zhang, W.; Long, E. Feasibility Experiment on the Simple Hot Box-Heat Flow Meter Method and the Optimization Based on Simulation Reproduction. *Appl. Therm. Eng.* **2015**, *83*, 48–56. [CrossRef]
20. Glavaš, H.; Hadzima-Nyarko, M.; Buljan, I.H.; Barić, T. Locating Hidden Elements in Walls of Cultural Heritage Buildings by Using Infrared Thermography. *Buildings* **2019**, *9*, 32. [CrossRef]
21. Evangelisti, L.; Scorza, A.; Vollaro, R.D.L.; Sciuto, S.A. Comparison between Heat Flow Meter (HFM) and Thermometric (THM) Method for Building Wall Thermal Characterization: Latest Advances and Critical Review. *Sustainability* **2022**, *14*, 693. [CrossRef]
22. Teni, M.; Krstić, H.; Kosiński, P. Review and Comparison of Current Experimental Approaches for In-Situ Measurements of Building Walls Thermal Transmittance. *Energy Build.* **2019**, *203*, 109417. [CrossRef]
23. Soares, N.; Martins, C.; Gonçalves, M.; Santos, P.; da Silva, L.S.; Costa, J.J. Laboratory and In-Situ Non-Destructive Methods to Evaluate the Thermal Transmittance and Behavior of Walls, Windows, and Construction Elements with Innovative Materials: A Review. *Energy Build.* **2019**, *182*, 88–110. [CrossRef]
24. Bienvenido-Huertas, D.; Moyano, J.; Marín, D.; Fresco-Contreras, R. Review of in Situ Methods for Assessing the Thermal Transmittance of Walls. *Renew. Sustain. Energy Rev.* **2019**, *102*, 356–371. [CrossRef]
25. Gaši, M.; Milovanović, B.; Gumbarević, S. Comparison of Infrared Thermography and Heat Flux Method for Dynamic Thermal Transmittance Determination. *Buildings* **2019**, *9*, 132. [CrossRef]
26. Komarizadehasl, S.; Khanmohammadi, M. Novel Plastic Hinge Modification Factors for Damaged RC Shear Walls with Bending Performance. *Adv. Concr. Constr.* **2021**, *12*, 355–365. [CrossRef]

27. Esfandiari, M.; Zaid, S.M.; Ismail, M.A.; Hafezi, M.R.; Asadi, I.; Mohammadi, S. A Field Study on Thermal Comfort and Cooling Load Demand Optimization in a Tropical Climate. *Sustainability* **2021**, *13*, 12425. [CrossRef]
28. Kim, S.H.; Kim, J.H.; Jeong, H.G.; Song, K.D. Reliability Field Test of the Air-Surface Temperature Ratio Method for in Situ Measurement of U-Values. *Energies* **2018**, *11*, 1. [CrossRef]
29. TESTO. TESTO. Available online: https://www.testo.com/es-MX/testo-435-1/p/0560-4351 (accessed on 1 February 2022).
30. Vučićević, B.; Turanjanin, V.; Bakić, V.; Jovanović, M.; Stevanović, Ž. Experimental and Numerical Modelling of Thermal Performance of a Residential Building in Belgrade. *Therm. Sci.* **2009**, *13*, 245–252. [CrossRef]
31. Andargie, M.S.; Azar, E. An Applied Framework to Evaluate the Impact of Indoor Office Environmental Factors on Occupants' Comfort and Working Conditions. *Sustain. Cities Soc.* **2019**, *46*, 101447. [CrossRef]
32. Evangelisti, L.; Guattari, C.; Gori, P.; de Lieto Vollaro, R.; Asdrubali, F. Experimental Investigation of the Influence of Convective and Radiative Heat Transfers on Thermal Transmittance Measurements. *Int. Commun. Heat Mass Transf.* **2016**, *78*, 214–223. [CrossRef]
33. Komarizadehasl, S.; Mobaraki, B.; Lozano-Galant, J.A.; Turmo, J. Development of a Low-Cost System for the Accurate Measurement of Structural Vibrations. *Sensors* **2021**, *21*, 6191. [CrossRef]
34. Porras Soriano, R.; Mobaraki, B.; Lozano-Galant, J.A.; Sanchez-Cambronero, S.; Prieto Muñoz, F.; Gutierrez, J.J. New Image Recognition Technique for Intuitive Understanding in Class of the Dynamic Response of High-Rise Buildings. *Sustainability* **2021**, *13*, 3695. [CrossRef]
35. Mobaraki, B.; Lozano-Galant, F.; Soriano, R.P.; Pascual, F.J.C. Application of Low-Cost Sensors for Building Monitoring: A Systematic Literature Review. *Buildings* **2021**, *11*, 336. [CrossRef]
36. Scislo, L.; Szczepanik-Scislo, N. Air Quality Sensor Data Collection and Analytics with IoT for an Apartment with Mechanical Ventilation. In Proceedings of the 2021 11th IEEE International Conference on Intelligent Data Acquisition and Advanced Computing Systems: Technology and Applications (IDAACS), Cracow, Poland, 22–25 September 2021; Volume 2, pp. 932–936. [CrossRef]
37. Saini, J.; Dutta, M.; Marques, G. Indoor Air Quality Monitoring Systems Based on Internet of Things: A Systematic Review. *Int. J. Environ. Res. Public Health* **2020**, *17*, 4942. [CrossRef] [PubMed]
38. Pierleoni, P.; Conti, M.; Belli, A.; Palma, L.; Incipini, L.; Sabatini, L.; Valento, S.; Mercuri, M.; Concetti, R. IoT Solution Based on MQTT Protocol for Real-Time Building Monitoring. In Proceedings of the IoT Solution Based on MQTT Protocol for Real-Time Building Monitoring, Ancona, Italy, 19–21 June 2019; pp. 57–62.
39. Mitro, N.; Krommyda, M.; Amditis, A. Smart Tags: IoT Sensors for Monitoring the Micro-Climate of Cultural Heritage Monuments. *Appl. Sci.* **2022**, *12*, 2315. [CrossRef]
40. Giusto, E.; Gandino, F.; Greco, M.L.; Grosso, M.; Montrucchio, B.; Rinaudo, S. An Investigation on Pervasive Technologies for IoT-Based Thermal Monitoring. *Sensors* **2019**, *19*, 663. [CrossRef]
41. Oztemel, E.; Gursev, S. Literature Review of Industry 4.0 and Related Technologies. *J. Intell. Manuf.* **2020**, *31*, 127–182. [CrossRef]
42. Ghosh, A.; Edwards, D.J.; Hosseini, M.R.; Al-Ameri, R.; Abawajy, J.; Thwala, W.D. Real-Time Structural Health Monitoring for Concrete Beams: A Cost-Effective 'Industry 4.0' Solution Using Piezo Sensors. *Int. J. Build. Pathol. Adapt.* **2021**, *39*, 283–311. [CrossRef]
43. Alarcón, M.; Martínez-García, F.M.; Gómez de León Hijes, F.C. Energy and Maintenance Management Systems in the Context of Industry 4.0. Implementation in a Real Case. *Renew. Sustain. Energy Rev.* **2021**, *142*, 110841. [CrossRef]
44. Aheleroff, S.; Xu, X.; Lu, Y.; Aristizabal, M.; Pablo Velásquez, J.; Joa, B.; Valencia, Y. IoT-Enabled Smart Appliances under Industry 4.0: A Case Study. *Adv. Eng. Informatics* **2020**, *43*, 101043. [CrossRef]
45. Martín-Garín, A.; Millán-García, J.A.; Baïri, A.; Millán-Medel, J.; Sala-Lizarraga, J.M. Environmental Monitoring System Based on an Open Source Platform and the Internet of Things for a Building Energy Retrofit. *Autom. Constr.* **2018**, *87*, 201–214. [CrossRef]
46. Ali, A.S.; Cote, C.; Heidarnejad, M.; Stephens, B. Elemental: An Open-Source Wireless Hardware and Software Platform for Building Energy and Indoor Environmental Monitoring and Control. *Sensors* **2019**, *19*, 4017. [CrossRef]
47. Mesas-Carrascosa, F.J.; Verdú Santano, D.; de Larriva, J.E.M.; Ortíz Cordero, R.; Hidalgo Fernández, R.E.; García-Ferrer, A. Monitoring Heritage Buildings with Open Source Hardware Sensors: A Case Study of the Mosque-Cathedral of Córdoba. *Sensors* **2016**, *16*, 1620. [CrossRef] [PubMed]
48. Echarri, V.; Espinosa, A.; Rizo, C. Thermal Transmission through Existing Building Enclosures: Destructive Monitoring in Intermediate Layers versus Non-Destructive Monitoring with Sensors on Surfaces. *Sensors* **2017**, *17*, 2848. [CrossRef] [PubMed]
49. Andújar Márquez, J.M.; Martínez Bohórquez, M.Á.; Gómez Melgar, S. A New Metre for Cheap, Quick, Reliable and Simple Thermal Transmittance (U-Value) Measurements in Buildings. *Sensors* **2017**, *17*, 2017. [CrossRef] [PubMed]
50. Serroni, S.; Arnesano, M.; Pandarese, G.; Martarelli, M.; Marco Revel, G. IoT Infrared Sensor for Continuous Monitoring of Building Envelope Thermal Performances. In Proceedings of the 2021 6th International Conference on Smart and Sustainable Technologies (SpliTech), Bol and Split, Croatia, 8–11 September 2021; pp. 1–6. [CrossRef]
51. Melexis. MLX90614. Available online: https://www.mouser.es/new/melexis/melexis-mlx90640-fir-sensor/ (accessed on 1 February 2022).
52. Maxim. MAX30205. Available online: https://www.maximintegrated.com/en/products/sensors/MAX30205.html?s_kwcid= AL!8732!3!517495051369!!!g!!&utm_source=google&utm_campaign=corp-sensors&gclid=Cj0KCQjwpv2TBhDoARIsALBnVnm _amL18iRn8n5HNoSnv1S72xQDIcsQ3LC3Uu9jJ-5eyE4J6pXtiZYaAoBJEALw_wcB (accessed on 1 February 2022).

53. FocuSens. DS18B20. Available online: https://www.focusensing.com/digital-temperature-sensor-assembly_c27?gclid=Cj0KCQ jwpv2TBhDoARIsALBnVnlly-N0z4pRiU80aYE2_utq7vwTNh6VUg3m_SN4mfYsA_hex9Mb7wcaApiYEALw_wcB (accessed on 1 February 2022).

54. Nepomuceno, M.C.S.; Martins, A.M.T.; Pinto, H.A.S. A Comparison between On-Site Measured and Estimated Based Adjustment Factor Values Used to Calculate Heat Losses to Unconditioned Spaces in Dwellings. *Buildings* **2022**, *12*, 146. [CrossRef]

55. ISO. ISO 6946:2017. Available online: https://www.iso.org/standard/65708.html (accessed on 1 February 2022).

56. ISO. ISO 9869:2014. Available online: https://www.iso.org/standard/59697.html#:~{}:text=ISO9869-1%3A2014describes,nosigni ficantlateralheatflow (accessed on 1 February 2022).

57. ISO. ISO 14813-1:2015. Available online: https://www.iso.org/standard/57393.html (accessed on 1 February 2022).

58. ISO. ISO 10456:2007. Available online: https://www.iso.org/standard/40966.html (accessed on 1 February 2022).

59. Afsar, M.M.; Tayarani-N, M.H. Clustering in Sensor Networks: A Literature Survey. *J. Netw. Comput. Appl.* **2014**, *46*, 198–226. [CrossRef]

60. Karagulian, F.; Barbiere, M.; Kotsev, A.; Spinelle, L.; Gerboles, M.; Lagler, F.; Redon, N.; Crunaire, S.; Borowiak, A. Review of the Performance of Low-Cost Sensors for Air Quality Monitoring. *Atmosphere* **2019**, *10*, 506. [CrossRef]

61. Lee, M.; Yoo, M. Characteristic of Thin-Film NTC Thermal Sensors. *Proc. IEEE Sensors* **2002**, *1*, 56–61. [CrossRef]

62. Tejero-Gómez, J.A.; Bayod-Rújula, A.A. Energy Management System Design Oriented for Energy Cost Optimization in Electric Water Heaters. *Energy Build.* **2021**, *243*, 111012. [CrossRef]

63. Abu Bakar, A.; Rahim, S.S.A.; Razali, A.R.; Noorsal, E.; Radzali, R.; Abd Rahim, A.F. Wearable Heart Rate and Body Temperature Monitoring Device for Healthcare. *J. Phys. Conf. Ser.* **2020**, *1535*, 012002. [CrossRef]

64. Enkhzul, D.; Erdenechimeg, D.; Amartuvshin, T.; Chuluunbaatar, N.; Enkhbaatar, T. *Implementation of Early Diagnostic Device for Diabetic Foot Using the Thermal Sensor*; University of Orléans: Orléans, France, 2016.

65. Wu, Y.; Liu, H.; Li, B.; Kosonen, R. Prediction of Thermal Sensation Using Low-Cost Infrared Array Sensors Monitoring System. In *IOP Conference Series: Materials Science and Engineering*; Institute of Physics Publishing: Bristol, UK, 2019; Volume 609. [CrossRef]

66. Kampezidou, S.I.; Ray, A.T.; Duncan, S.; Balchanos, M.G.; Mavris, D.N. Real-Time Occupancy Detection with Physics-Informed Pattern-Recognition Machines Based on Limited CO_2 and Temperature Sensors. *Energy Build.* **2021**, *242*, 110863. [CrossRef]

67. Mobaraki, B.; Komarizadehasl, S.; Castilla, F.J.; Lozano-Galant, J.A. Open Source Platforms for Monitoring Thermal Parameters of Structures. In *Bridge Maintenance, Safety, Management, Life-Cycle Sustainability and Innovations*; CRC Press: Boca Raton, FL, USA, 2019; pp. 3892–3896.

68. Wu, L.H.; Yao, J.Y.; Lin, X.R.; Zhang, H.Y. Design of Acquisition and Control System of Granary Supervisory Control and Data Acquisition System. *Int. J. Multimed. Ubiquitous Eng.* **2015**, *10*, 1–8. [CrossRef]

69. Zhan, Q.; Pungercar, V.; Musso, F.; Ni, H.; Xiao, Y. Hygrothermal Investigation of Lightweight Steel-Framed Wall Assemblies in Hot-Humid Climates: Measurement and Simulation Validation. *J. Build. Eng.* **2021**, *42*, 103044. [CrossRef]

70. Ibrahim, M.; Moselhi, O. Inertial Measurement Unit Based Indoor Localization for Construction Applications. *Autom. Constr.* **2016**, *71*, 13–20. [CrossRef]

71. Moschevikin, A.P.; Sikora, A.; Lunkov, P.V.; Fedorov, A.A.; Maslennikov, E.I. Hardware and Software Architecture of Multi Mems Sensor Inertial Module. In Proceedings of the 2017 24th Saint Petersburg International Conference on Integrated Navigation Systems (ICINS), St. Petersburg, Russia, 29–31 May 2017; pp. 7–9. [CrossRef]

72. Nuhu, B.K.; Aliyu, I.; Adegboye, M.A.; Ryu, J.K.; Olaniyi, O.M.; Lim, C.G. Distributed Network-Based Structural Health Monitoring Expert System. *Build. Res. Inf.* **2021**, *49*, 144–159. [CrossRef]

73. Scietec. TNP006. Available online: https://scitec.uk.com/irsources/index?ppc_keyword=ir (accessed on 1 February 2022).

74. Sensirion. SHT35. Available online: https://sensirion.com/products/catalog/SHT35-DIS-F/ (accessed on 1 February 2022).

75. Arduino.cc. Arduino MEGA. Available online: http://store.arduino.cc/products/arduino-mega-2560-rev3 (accessed on 1 February 2022).

76. Komarizadehasl, S.; Mobaraki, B.; Ma, H.; Lozano-Galant, J.-A.; Turmo, J. Low-Cost Sensors Accuracy Study and Enhancement Strategy. *Appl. Sci.* **2022**, *12*, 3186. [CrossRef]

77. Instrument, T. TCA9548A. Available online: https://www.ti.com/product/TCA9548A?utm_source=google&utm_medium=cpc &utm_campaign=asc-int-null-prodfolderdynamic-cpc-pf-google-wwe&utm_content=prodfolddynamic&ds_k=DYNAMIC+ SEARCH+ADS&DCM=yes&gclid=Cj0KCQjwpv2TBhDoARIsALBnVnmCDY4fUb5wjVwsB2l-XinVxE2ofvGlqBtLYe5vFUIZw ikHZjzrzosaAiJGEALw_wcB&gclsrc=aw.ds (accessed on 1 February 2022).

78. Last Minute Engineer. DS3231. Available online: https://www.focusensing.com/digital-temperature-sensor-assembly_c27?gcli d=Cj0KCQjwpv2TBhDoARIsALBnVnlly-N0z4pRiU80aYE2_utq7vwTNh6VUg3m_SN4mfYsA_hex9Mb7wcaApiYEALw_wcB (accessed on 1 February 2022).

79. Matworks. MatLab. Available online: https://www.mathworks.com/ (accessed on 1 February 2022).